The physics of wave-coupling in low-frequency plasma heating

Kurt Appert, T. Hellsten, Hinrich Lütjens, Olivier Sauter, Jan Vaclavik, Laurent Villard

April 1987 LRP 319/87

THE PHYSICS OF WAVE-COUPLING IN LOW-FREQUENCY PLASMA HEATING

K. Appert, T. Hellsten, H. Lütjens, O. Sauter,
J. Vaclavik and L. Villard

Invited Paper presented at the

**1987 International Conference on Plasma Physics
Kiev, USSR - April 6-12, 1987**

by
K. Appert

THE PHYSICS OF WAVE-COUPLING IN LOW-FREQUENCY PLASMA HEATING

K. Appert, T. Hellsten*. H. Lütjens, O. Sauter, J. Vaclavik
and L. Villard

Centre de Recherches en Physique des Plasmas
Association Euratom - Confédération Suisse
Ecole Polytechnique Fédérale de Lausanne
21, Av. des Bains, CH-1007 Lausanne/Switzerland

* JET Joint Undertaking, Abingdon, Great Britain

ABSTRACT

Recent developments of the hot plasma theory involving non-zero equilibrium gradients are discussed in the basic context of energy conservation. The corresponding boundary value problems are formulated in variational form and solved by the finite element method. This method is shown to lead to transparent and reliable numerical models. Basic physics questions are addressed in both the Alfvén Wave and the Ion-Cyclotron Range of Frequencies.

1. INTRODUCTION

The excitation of small-amplitude electromagnetic waves in a plasma can be treated theoretically by two very different methods: the geometric optics approximation or the resonant cavity assumption.

In the Alfvén Wave Range of Frequencies (AWRF) that is at very low frequencies, one must assume a resonant cavity, whereas in the Electron Cyclotron Range of Frequencies that is at very high frequencies, the geometric optics is the ideal tool. In the intermediate frequency ranges at the ion cyclotron (ICRF) and the lower hybrid frequencies both methods have advantages and disadvantages. As one goes to lower frequencies and smaller devices the resonant cavity assumption becomes more and more appropriate but even in large devices

like JET ICRF cavity modes have been observed.[1] In the present work we concentrate on the resonant cavity assumption; concerning the geometric optics approximation, we refer the reader to a recent review by Brambilla.[2]

The present authors have already reviewed the theory of MHD waves[3] based on the resonant cavity assumption and relevant to low frequency plasma heating (AWRF, ICRF). The stress of that discussion was on cold and resistive plasma models and resonance absorption. The present paper can be regarded as a followup of Ref. 3 as it concentrates on non-ideal aspects in the theory, like temperature or finite electron mass. What has merely been described as resonance absorption in Ref. 3 will now be treated as linear mode conversion at least in one dimension. The paper is, however, not a review of the kinetic theory of wave excitation at low frequencies but a contribution to its further development. Investigating by numerical means the role played in theory by equilibrium gradients[4] we are able to treat on the same footing plane slab and cylindrical plasmas, AWRF and ICRF, and all the relevant collisionless dissipation mechanisms including transit time magnetic pumping by standing waves. This goes partly beyond previous work in the AWRF[5-10] and in the ICRF.[11-16]

We find that the terms in the dielectric tensor proportional to the ratio between the Larmor radius and the equilibrium scale-length show the route to a satisfactory definition of the local absorption of an electromagnetic wave in a hot magnetized plasma. To first order in Larmor radius the so-defined local absorption is identical to that obtained ad hoc by McVey and co-workers[17] and by Vaclavik and Appert using a more rigorous approach.[18]

For our theoretical investigation it is essential that we may treat the wave equation

$$\mathrm{rot}\,\mathrm{rot}\,\vec{E} = \frac{\omega^2}{c^2}\,\vec{\vec{\varepsilon}}\cdot\vec{E}, \qquad \vec{E} \sim e^{-i\omega t} \tag{1}$$

as it stands with all the odds and ends where $\vec{E}$ is the wave electric field, $\vec{\vec{\varepsilon}}$ the dielectric tensor operator, c the speed of light and ω the wave frequency, respectively. The method of numerical physics

enabling us to do so is described in Chap. II. In Chapter III we mention the hot plasma wave equation, the boundary conditions under which it is solved and discuss conservation laws and local absorption. In Chapter IV we review the wave excitation phenomena in the AWRF using a cylindrical model. Finally, in Chap. V, using both kinetic plane slab and cold-plasma toroidal models we try to get some insight into the linear mode conversion in the ICRF.

2. A METHOD OF NUMERICAL PHYSICS FOR LINEAR WAVE PROPAGATION

A conceptually extremely simple method for the numerical solution of ordinary and partial differential equations is the Finite Element Method (FEM). Given a linear differential equation in the spatial domain G

$$\mathcal{L} U = 0 \tag{2}$$

together with appropriate boundary conditions on δG, one searches for approximate solutions of the form

$$U(\vec{x}) \approx u(\vec{x}) = \sum_{j=1}^{N} u_j \Psi_j(\vec{x}). \tag{3}$$

The method is called FEM because the basis functions $\Psi_j(\vec{x})$ have a finite support based on some subdivision (finite element discretisation) of the solution domain G. The most commonly used way to determine the unknown coefficients u_j in Eq. (3) starts from the Galerkin weak variational form[19] of Eq. (2),

$$\int_G V \mathcal{L} U \, d\vec{x} = 0, \quad \forall V, \tag{4}$$

where V is an appropriate test function. One usually integrates $\mathcal{L}$ by parts until V and U are subject to roughly the same order of differentiation. During this partial integration some of the boundary conditions can be used and become natural boundary conditions of the variational problem. Those conditions which cannot be used at that time are

essential conditions and must be imposed explicitely on $u(\vec{x})$, Eq. (3).

If the basis functions Ψ_j are used as test functions as well - which one commonly does - the approximate form of Eq. (4) becomes

$$\sum_j \int_G \Psi_i \hat{\mathcal{L}} \Psi_j \, d\vec{x} \, u_j = \text{surface terms}, \quad \forall \, i = 1, \ldots, N, \qquad (5)$$

where by $\hat{\mathcal{L}}$ we mean the operator which, after partial integration of $\mathcal{L}$, acts to the left and to the right. Equation (5) is a set of N algebraic equations for the N unknowns u_j. In one dimension this method has the disadvantage of needing more computer memory and programming skills than a straightforward shooting method like a Runge-Kutta integration but it works, in contrast to the latter, under all imaginable situations. In particular, one can easily deal with the stiff problem of strongly evanescent waves.[20]

In most of RF heating scenarios in inhomogeneous plasmas there exist some wave modes which are strongly evanescent in certain parts of the solution domain: the FEM makes a global solution possible; no subdivision into domains with different physical parameters is needed. This, in turn, enables one to separate in the computer code the solution algorithm from the physics, represented by the dielectric tensor. Hence the code can be modular and transparent which are essential qualities of a reliable numerical tool. The dielectric tensor is defined at one and only one place in the code. It is therefore easy to investigate changes in the physics by changing the dielectric tensor. This feature of the numerical method was particularly important in our investigation of different energy conserving forms of the wave equation.

When applying the FEM to eq. (1), one does not eliminate any component of $\vec{E}$ unless one uses the restricted physical model where $E_z = 0$. This procedure has several essential advantages over the elimination procedures leading to higher order equations.[11] First of all, as one does nothing, one does not introduce errors. Secondly, the code remains transparent because one deals directly with the Eq. (1).

Thirdly, no equilibrium gradients appear unless they are introduced explicitly into the dielectric tensor. Last but not least, it is an advantage to obtain standardly all components of the electric field. In some versions of our kinetic codes we have even gone so far as to compute all components of the electric and the magnetic fields, $\vec{E}$ and $\vec{B} = -i(c/\omega)\mathrm{rot}\ \vec{E}$, and the particle number and current densities, n_ℓ and $\vec{j}_\ell$, respectively. The latter quantities can be obtained for each species ℓ from the dielectric tensor or rather from the susceptibility $\vec{\vec{\chi}}_\ell$,

$$\vec{j}_\ell = -i(\omega/4\pi)\ \vec{\vec{\chi}}_\ell \cdot \vec{E}, \tag{6}$$

$$n_\ell = (1/i\omega q_\ell)\ \mathrm{div}\ \vec{j}_\ell \tag{7}$$

Equation (6) is also evaluated by the FEM. Ampère's law, Poisson's equation and $\mathrm{div}\vec{B} = 0$ can then serve as tests for the coding. These tests combined with convergence studies[20] also evidence the reliability of the numerical method.

In practice, one uses piecewise constant, piecewise linear or piecewise cubic functions in the approximation, Eq. (3). For details concerning the numerical analysis we refer the reader to the specialized literature.[19-21]

3. THE HOT-PLASMA MODEL

To demonstrate some problems one may encounter with the hot-plasma model, we start to discuss the wave equation describing small amplitude electromagnetic perturbations in a plane, hot, non-uniformly magnetized ($B_0 = B_0(x)e_z$), inhomogeneous plasma. Expanding the Vlasov and Maxwell equations to second order in the smallness of the Larmor radius compared to characteristic scale-lengths of the plasma and fields, Martin and Vaclavik[4] have derived the dielectric tensor operator for a wave motion of the form

$$\vec{E}(x)\, e^{i(k_y y + k_z z - \omega t)} \tag{8}$$

In a closed form their tensor includes Čerenkov, fundamental and first harmonic cyclotron interactions together with all the equilibrium gradient terms up to second order. To our knowledge the complete tensor operator has never been given explicitely before Ref. 4.

As one would expect, we have found that most of the equilibrium gradient terms are negligible in many situations especially in the ICRF. In the AWRF where the characteristic scale-lengths of the plasma may be of the same order as those of the field some gradient terms are important. Although the gradients seem to influence hardly the solution of the wave equation (1) in the ICRF, they can influence, however, the interpretation of what one regards as the <u>local</u> power absorption.

The dielectric tensor given in Ref. 4 has the form

$$\vec{\vec{\epsilon}} = \vec{\vec{\gamma}} + \vec{\vec{\beta}}^{-}\frac{d}{dx} + \frac{d}{dx}\vec{\vec{\beta}}^{+} + \frac{d}{dx}\vec{\vec{\alpha}}\frac{d}{dx} \,. \tag{9}$$

The operators d/dx act on everything to their right. The tensors $\vec{\vec{\alpha}}$ and $\vec{\vec{\gamma}}$ have the following symmetry properties

$$-\gamma_{xy} = \gamma_{yx}\,, \quad -\gamma_{xz} = \gamma_{zx}\,, \quad \gamma_{yz} = \gamma_{zy}\,, \tag{10}$$

where, however, $\alpha_{xz} = \alpha_{yz} = 0$. The tensors $\vec{\vec{\beta}}^{+}$ and $\vec{\vec{\beta}}^{-}$ have the structure

$$\vec{\vec{\beta}}^{-} = \begin{pmatrix} 0 & \beta^{-}_{xy} & \beta^{-}_{xz} \\ 0 & 0 & \beta^{-}_{yz} \\ 0 & 0 & 0 \end{pmatrix}, \quad \vec{\vec{\beta}}^{+} = \begin{pmatrix} 0 & 0 & 0 \\ \beta^{-}_{xy} & 0 & 0 \\ \beta^{-}_{xz} & -\beta^{-}_{yz} & 0 \end{pmatrix}. \tag{11}$$

The particular form of the tensor elements is not of interest here and can be found in Ref. 4. We mention, however, that β^{-}_{xy} contains first order gradient terms and $\vec{\vec{\gamma}}$ first and second order terms.

If we restrict ourselves to first order gradients of the particle densities and temperatures we may write

$$\vec{\vec{\gamma}} = \vec{\vec{\epsilon}}^{(0)} + \left(\frac{d\vec{\vec{\eta}}}{dx}\right), \tag{12}$$

where $\vec{\vec{\epsilon}}^{(0)}$, the classical[22] dielectric tensor, and $\vec{\vec{\eta}}$ can be inferred from Ref. 4. Replacing $\vec{\vec{\gamma}}$ by Eq. (12) one finds the following dielectric operator

$$\vec{\vec{\epsilon}} = \vec{\vec{\epsilon}}^{(0)} + \vec{\vec{b}}^{-}\frac{d}{dx} + \frac{d}{dx}\vec{\vec{b}}^{+} + \frac{d}{dx}\vec{\vec{\alpha}}\frac{d}{dx} \tag{13}$$

where $\vec{\vec{b}}^{-} = \vec{\vec{\beta}}^{-} - \vec{\vec{\eta}}$ and $\vec{\vec{b}}^{+} = \vec{\vec{\beta}}^{+} + \vec{\vec{\eta}}$. This trivial remodelling of $\vec{\vec{\epsilon}}$ has non-trivial consequences on the interpretation of the conservation laws derivable from Eq. (1),

$$\frac{d}{dx}(S + S_T) + Q = 0. \tag{14}$$

Here S is the time-averaged x-component of the Poynting vector,

$$S_T = \frac{\omega}{8\pi}\,\mathrm{Im}\,\vec{E}^{*}\cdot\left[\vec{\vec{\alpha}}\frac{d}{dx} + \vec{\vec{b}}^{+}\right]\cdot\vec{E} \tag{15}$$

and

$$Q = \frac{\omega}{8\pi}\,\mathrm{Im}\left[-\frac{d\vec{E}^{*}}{dx}\cdot\left(\vec{\vec{\alpha}}\frac{d}{dx} + \vec{\vec{b}}^{+}\right) + \vec{E}^{*}\cdot\left(\vec{\vec{b}}^{-}\frac{d}{dx} + \vec{\vec{\epsilon}}^{(0)}\right)\right]\cdot\vec{E}. \tag{16}$$

Clearly, Eq. (14) cannot be declared to be the energy conservation law because the definition of S_T and Q, the thermal flux and the local energy absorption, is not unique. One can indeed define

another pair, $\hat{S}_T$ and $\hat{Q}$, by replacing in Eqs. (15) and (16) $\vec{\vec{b}}^+$ by $\vec{\vec{\beta}}^+$ and $\vec{\vec{b}}^-$ by $\vec{\vec{\beta}}^-$.[4] Yet other definitions can be obtained when some gradient terms are kept in $\vec{\vec{\gamma}}$. Only the remaining terms would then appear in the definition of S_T. If, in our argumentation, we would neglect the gradient terms altogether, we could introduce any arbitrary $\vec{\vec{\eta}}$ in Eq. (12) and arrive at any grotesque S_T and Q in Eqs. (15) and (16). The theory of wave propagation in a homogeneous plasma therefore cannot be of any help in the definition of the thermal flux and the local energy absorption.

In this bad situation resort has been taken to the most basic definition of energy absorption by particles.[17,18] Essentially one calculates the time average of

$$\frac{\partial}{\partial t}\int \frac{Mv^2}{2} f\, d^3v \qquad (17)$$

to second order in the wave field, Eq. (8). Here M, v and f denote particle mass, velocity and velocity distribution, respectively, Along these lines one arrives at a definition for the local power absorption, $Q^{(2)}$, which, upto first order in Larmor radius, is equal to Q as defined in Eq. (16). In a stable plasma $\hat{Q}(x)$ is positive definite unlike e.g. Q(x) defined on the basis of Eq. (9).

It seems therefore that the wave equation should not contain any explicit gradient term when it is used to define energy flux. Moreover, explicit gradient terms cause troubles at any finite-temperature or finite-density plasma boundary because they are unbounded in infinitely small transition layers. If, however, they are removed to the higher order (in d/dx) terms of the tensor $\vec{\vec{\varepsilon}}$, they are absolutely inoffensive and boundary conditions can be formulated by means of an integration over the boundary layer.[4,23] Consequently all the boundary conditions at the plasma-vacuum interface become natural conditions of the weak variational form, Eq. (5). As a further consequence, the same conditions can be used for the hot and the cold plasma models.[23]

As long as the temperature T approaches zero at the plasma boundary, the solution of Eq. (1) is not affected by the choice of $\vec{\vec{\varepsilon}}$, Eq. (9) or (13) respectively, because $\vec{\vec{\eta}} = 0$ for $T = 0$. In cylindrical geometry, however, T is finite on the axis and the boundary terms due to $\vec{\vec{\eta}}$ must be taken seriously. We have again found that the explicit gradient terms must be made implicit in the sense of Eq. (13).

For the cylindrical geometry it has been necessary to repeat the derivation of $\vec{\vec{\varepsilon}}$ in analogy to that of Ref. 4 because a few terms cannot be inferred from the plane slab geometry. As the assumption of a cylindrical symmetry is reasonable for the AWRF only, our derivation was limited to the Čerenkov interaction.

In the cylindrical geometry (r,θ,z) the dielectric tensor operator takes the form

$$\vec{\vec{\varepsilon}} = \vec{\vec{C}} + \vec{\vec{B}}^{-}\frac{d}{dr} + \frac{1}{r}\frac{d}{dr}r\vec{\vec{B}}^{+} + \frac{1}{r}\frac{d}{dr}r\vec{\vec{A}}\frac{d}{dr} \qquad (18)$$

when the wave field is $\vec{E}(r)\, e^{i(m\theta + kz - \omega t)}$. The tensors $\vec{\vec{A}}$, $\vec{\vec{B}}^{+}$, $\vec{\vec{B}}^{-}$ and $\vec{\vec{C}}$ can be obtained by first transforming $\vec{\vec{\alpha}}$, $\vec{\vec{\beta}}^{+}$, $\vec{\vec{\beta}}^{-}$ and $\vec{\vec{\varepsilon}}(o)$ into cylindrical coordinates and then adding (substracting) the following gradient terms to(from) the transformed $\vec{\vec{\beta}}^{+}(\vec{\vec{\beta}}^{-})$:

$$\begin{aligned} h_{\theta\theta} &= \tau/r, & h_{\theta z} &= k\tau, \\ h_{z\theta} &= k\sigma, & h_{zz} &= -\frac{m}{r}\sigma, \end{aligned} \qquad (19)$$

where

$$\begin{aligned} \tau &= \frac{v_{th}^2\,\omega_p^2}{\omega^2\,\omega_c^2}\,Z_o^s, \\ \sigma &= \frac{\omega_p^2}{\omega\,\omega_c\,k^2}\,(1 - Z_o^s). \end{aligned} \qquad (20)$$

Here $v_{th} = 2T/M$, ω_p and ω_c denote the thermal velocity, the plasma and the cyclotron frequency, respectively, and $Z_o^s = Z^s(\omega/|k_z|v_{th})$ is the plasma dispersion function as defined by

Shafranov.[24]

The so-defined dielectric tensor includes the magnetic pumping terms in $A_{\theta\theta}$ and $B_{\theta\theta}$ which is important for the damping of the Global Eigenmodes of the Alfvén Wave and of the Fast Magnetosonic Wave. In previous AWRF heating related work[5-10] magnetic pumping has been neglected.

In the derivation of eq. (18) we have assumed a purely axial equilibrium magnetic field, $\vec{B} = B_{0z}\vec{e}_z$, $B_{0z} = \text{const}$. We know, however, from all our previous investigations[3] using cold-plasma theory that the wave propagation and coupling in the AWRF is strongly influenced by the existence of an axial (toroidal) equilibrium current. A poloidal magnetic field $B_{0\theta}(r)$ is important even if $|B_{0\theta}/B_{0z}| \ll 1$ as in a tokamak. Using the smallness of $|B_{0\theta}/B_{0z}|$ we can transform $\vec{\varepsilon}$ in Eq. (18) into magnetic coordinates $\vec{e}_r$, $\vec{e}_\perp = \vec{e}_\parallel \times \vec{e}_r$, $\vec{e}_\parallel = \vec{B}_0/B_0$ by replacing m/r and k by

$$k_\perp = \left(B_{0z}\frac{m}{r} - B_{0\theta}k\right)/B_0$$

and (21)

$$k_\parallel = \left(B_{0\theta}\frac{m}{r} + B_{0z}k\right)/B_0 ,$$

and by identifying r, θ and z-components with r, $\perp$ and $\parallel$-components. The equilibrium current term λ has the form[25]

$$\lambda = -i\,\frac{c^2}{\omega^2}\,\frac{k_\parallel}{r}\,\frac{d}{dr}\left(\frac{r B_{0\theta}}{B_0}\right) \qquad (22)$$

and has to be added to $C_{r\perp}$ and to $-C_{\perp r}$. In Eq. (1) it combines with similar terms appearing in $(\text{rotrot}\vec{E})_r$ and $(\text{rotrot}\vec{E})_\theta$ in such a way that the gradients again disappear.

Now that the wave equations for the plane slab and cylindrical geometries are defined we shall briefly discuss the boundary conditions under which these equations are solved. Let us start with the axis in the cylindrical geometry. The regularity conditions at r = 0 are

$$E_r = E_\perp = dE_\parallel/dr = 0 \quad \text{for} \quad |m| \neq 1 \tag{23}$$

and

$$(E_r + imE_\theta) = \frac{d}{dr}(E_r + imE_\theta) = E_z = 0 \quad \text{for} \quad |m| = 1. \tag{24}$$

They are essential conditions and must be imposed at $r = r_0 \ll r_p$, where r_p is the plasma radius.

The situation at the axis strongly contrasts with that at the plasma-vacuum interface where all conditions are natural in nature. Irrespective of the geometry one can choose the solution domain G such that it includes the plasma "outer" boundary $r_p + 0$ where S_T, Eq. (15), can be assumed to be zero even if it is finite at the "inner" boundary, r_p-0. In this way one satisfies continuity conditions on $E_\perp$ and $E_\parallel$ (or E_y and E_z respectively) as well as the requirement that their derivatives be bounded.[4]

The weak variational form for the slab geometry is obtained from Eqs. (1) and (13):

$$\int_{-r_p-0}^{r_p+0} \left[\mathrm{rot}\vec{F}^* \cdot \mathrm{rot}\vec{E} - \frac{\omega^2}{c^2}\left(\vec{F}^* \cdot \vec{\vec{\epsilon}} \cdot \vec{E} + \vec{F}^* \cdot \vec{\vec{b}} \cdot \frac{d\vec{E}}{dx} - \frac{d\vec{F}^*}{dx} \cdot \vec{\vec{b}}^t \cdot \vec{E} - \right.\right.$$

$$\left.\left. \frac{d\vec{F}^*}{dx} \cdot \vec{\vec{\alpha}} \cdot \frac{d\vec{E}}{dx} \right) \right] dx = \left(\vec{F}^* \times \mathrm{rot}\vec{E} \right)_x \Big|_{-r_p-0}^{r_p+0} . \tag{25}$$

The test function $\vec{F}^*$ belongs to the same function space as $\vec{E}$, Eq. (8). The two surface terms $\vec{F}^* \times \mathrm{rot}\vec{E}$ are directly expressible via the wave magnetic field $\vec{B} \sim \mathrm{rot}\vec{E}$ at $x = \pm(r_p + 0)$.

In the usual RF heating models the plasma is surrounded by vacuum and conducting walls. Somewhere in the vacuum one places an antenna modelled by an infinitely thin current layer with or without radial feeders.[26] Irrespective of whether the displacement current is

neglected or not, one can solve for the wave fields in the vacuum either numerically or analytically. The so-obtained solution then serves to express rotE in terms of the antenna current and $\vec{E}$ at $\pm(r_p + 0)$.[23] The power emitted by the antenna is obtained from

$$P = \frac{1}{2} \int_{\text{vacuum}} d^3x \, \vec{j}_a \cdot \vec{E}^* \qquad (26)$$

where j_a denotes the antenna current.

The treatment of the vacuum in the cylindrical geometry and of the plasma-vacuum interface is a trivial variant of the corresponding plane case.

4. WAVE EXCITATION IN THE ALFVEN WAVE RANGE OF FREQUENCIES

We now turn to an investigation of the different waves which can be excited in the AWRF. The numerical tool we have at our disposition includes all the relevant physics in contrast to earlier models.[8-10,27] In particular, transit time magnetic pumping is included. The phenomenology of the excitation as described in earlier publications [5-10,27-28] is, however, not affected.

Extensive experimental investigations of wave excitation in the AWRF have been undertaken on the TCA tokamak at Lausanne.[29-30] For this reason we concentrate our computations on TCA. If not otherwise stated the antenna and plasma parameters used are the following: deuterium plasma, major and minor radius, R = 65 cm and r_p = 18 cm, toroidal (axial) and poloidal wave numbers n = -2 (k = -0.03 cm^{-3}), m = -1; exciting frequency, f_o = 3 MHz; number density of species ℓ, $n_{\ell o}(r) = n_{\ell o}(1.-0.98r^2/r_p^2)^{0.7}$; temperatures, $T_{\ell o}(r) = T_{\ell o}(1.-0.84r^2/r_p^2)^2$ with T_{eo} = 800 eV and T_{io} = 500 eV; toroidal (axial) magnetic field, B_{oz} = 1.5 T, plasma current density, $j_{oz}(r) = j_{oz}(1-r^2/r_p^2)^2$ with an amplitude j_{oz} such that the total current is 120 kA. As a result of these parameters the safety factor has the values, q(0) = 1 and $q(r_p)$ = 3.

In Fig. 1 is shown the power, Eq. (26), versus the electron density on axis. In its very first part, $2 \cdot 10^{13} \leq n_{eo} \leq 9 \cdot 10^{13}$ cm^{-3}, the graph corresponds to the experimental antenna loading measurements in TCA.[29] Higher densities are outside the usual operational domain for heating experiments on TCA and are shown for academic reasons. As in the axisymmetric case[10] one can distinguish essentially four different excitation conditions denoted by GEAW, KAW, CONT and SQEW. At the lowest density, $n_{eo} = 2.61 \cdot 10^{13}$ cm^{-3}, the plasma responds with a high quality eigenmode, the fundamental Global Eigenmode of the Alfvén Wave (GEAW). Having its frequency outside the cold plasma continuum, this mode can correctly be situated even with a cold plasma model.[25] The quality (height) of the response, however, can only be obtained from the hot plasma theory, including magnetic pumping. The magnetic pumping increases the height of the peak by 50% over that obtained without pumping. From a theorist's point of view this is a large correction. When put into the experimental context, however, the correction is quite irrelevant because the experimentally observed responses[29] have never the high quality of the GEAW in Fig. 1.

The next peak denoted by KAW (Kinetic Alfvén Wave) is situated in the range of the cold plasma continuum and cannot be found there with a cold plasma model. On the contrary, the latter model would predict an infinity of GEAW's between the actual GEAW and the continuum edge, i.e. between GEAW and KAW. In the present case (n = -2), only the fundamental GEAW survives the finite temperature corrections in the kinetic model; in the case n = -1 the first and the second GEAW can survive. It is reasonable to call the wave motion inside the continuum the Kinetic Alfvén Wave[5] although in a kinetic model there is no fundamental difference between the GEAW and the KAW: they are just the fundamental and higher radial eigenmodes of the Alfvén wave. Their excitation is facilitated by the existence of a low quality compressional motion with collective mode character, the MHD surface wave mode.[31]

The KAW manifests itself as long as it exhibits an appreciable field amplitude on the axis, Fig. 2. At higher densities, indicated by CONT (continuum) in Figs. 1 and 2, the kinetic Alfvén wave does not

reach the centre and, hence, cannot set up an eigenmode. For Fig. 2 we have chosen E_r rather than E or $E_\parallel$ because E_r exhibits both the cold and the hot plasma features and also some problems of theoretical nature near the boundary.

Let us now turn to high densities or to the excitation of kinetic waves near the boundary, respectively. Donnelly at al.[10] have termed the wave excited in the cold plasma near the boundary the "surface electrostatic wave". We prefer to call it the Surface Quasi Electrostatic Wave (SQEW) because the compressibility plays an important role in its excitation. The SQEW form shown in Fig. 2 exhibits one main hump with a short wavelength superposed. The main hump is the SQEW whereas the short wavelength, which is of the order of the ion Larmor radius, corresponds to the third solution of the dispersion relation obtained from Eq. (1) and is unphysical. The existence of this unphysical wave mode is the price we have to pay for our general approach where we do not eliminate $E_\parallel$ using some approximations. So far it seems that this mode does not interfere at all with the rest of the physics. It is excited at the boundary and damped within 2 cm. In particular, it does not affect the energy deposition density.[32] We have even the hope to make it disappear altogether by working up to second order in the equilibrium gradients in analogy to Eq. (13). A pragmatical approach which makes it disappear is to introduce electron-ion collisions (ν_{ei}) in $\varepsilon^{(0)}_{zz}$, i.e.

$$\varepsilon^{(0)}_{zz} \longrightarrow \varepsilon^{(0)}_{zz} + \frac{\omega_{pe}^2}{\omega^2}\left(1 - \frac{1}{1 + i\nu_{ei}/\omega}\right), \qquad (27)$$

and to decrease the electron temperature to 2 eV at boundary instead of 20 eV as in Fig. 2. In any event we do not attach too much importance to the physics in the boundary layer because experimentally it is found to be highly turbulent, an aspect we theoretically do not model at all. Some interesting results have been reported in Ref. 28.

In Fig. 3 we show how the distance (in density) between the first two peaks (i.e. GEAW and KAW in Fig. 1) varies with toroidal mode

number and current. The current and its profile have been varied in such a way that $q(0) = 1$. The temperature on axis has also been varied and was found to be a quantity of little influence. The values of the relative distance $\Delta n_{eo}/n_{eo}$ are of the same order as those found experimentally.[33] A detailed comparison using experimental current and density profiles should be undertaken and could well reveal a certain potential for diagnostics.[34]

In contrast to Fig. 1 we show in Fig. 4 a loading trace in the experimentally relevant density range. Here the four dominant modes $m = \pm 1$ and $n = \pm 2$ have been summed. Two different values of the temperature at the plasma boundary have been used $T \sim (1-0.84r^2/r_p^2)^2$ and $(1-0.95r^2/r_p^2)^2$. We see that the peaks due to the GEAW and the KAW are hardly affected by the temperature whereas those due to the SQEW $(m,n) = (-1,2), (1,-2)$ disappear with the higher temperature. At $T_{eo}(r_p) = 2$ eV the introduction of electron-ion collisions makes them disappear too. From a theoretical point of view it seems therefore that the SQEW has no clear signature in TCA when excited with 3 MHz. It could, however, be responsible for some of the background loading observed.[29] Whenever excited in our numerical models it is excited via mode conversion from the compressional mode and not by direct antenna coupling.[35] For a given pair (m,n) its excitation seems not to depend on the direction of the antenna current which can be varied in our model. We shall obtain more insight into these questions when higher frequencies will be used on TCA.

In Fig. 5 we show the parallel component of the wave magnetic field in the vacuum adjacent to the plasma. The parameters are those of Fig. 4. Particularly interesting is the fact that the phase goes through 4π when the GEAW and KAW are excited. Phase jumps as high as 6π have been observed on TCA[30] and may be interpreted as a signature of the GEAW and KAW.

So far in our discussion we did not consider toroidal and other geometric effects. Generally, in the AWRF they lead to weak coupling between eigenmodes of the idealized cylindrical geometry with one noticeable exception, the GEAW $m = 0$ which does not exist in cylin-

drical geometry.[36] In ICRF, on the other hand, the geometry is dominated by the $\omega = \omega_{ci}(r)$ line and a plane slab model is the only one-dimensional (1D) model possible. The transition from a 1D to a two-dimensional (2D) toroidal model is easy to understand in the AWRF but not in the ICRF. The latter transition is the subject of the next chapter.

5. WAVE EXCITATION IN THE ION CYCLOTRON RANGE OF FREQUENCIES

Around the world there are several 2D kinetic ICRF codes in development. So far basic plasma physics questions have not been addressed with these codes. One of the most basic questions is that concerning linear mode conversion in 2D: where and how is the fast magnetosonic wave converted into the kinetic wave. Here, we shall try to infer the 2D hot plasma conversion physics from the kinetic 1D model described in Ch. 3 (but with $E_\parallel = 0$) and from the cold plasma 2D model LION.[21]

We start with a review of the well-known phenomenon of mode conversion in one dimension.[37,26] The first discussion is based on a TCA like plasma. The changes with respect to Ch. 4 are: $n = 4$, $f_o = 22$ MHz, deuterium/hydrogen mixture $n_{D0} = 10^{13}$ cm^{-3}, $n_{H0} = 10^{12}$ cm^{-3} with parabolic profiles. With these parameters the cold-plasma wave equation is singular near the axis at the ion-ion hybrid resonance. Physically this resonance corresponds to the spatial location x of a singular Alfvén or ion-cyclotron eigenmode with an eigenfrequency ω_A equal to the driving frequency, $\omega_A(x) = \omega$. In an initial value approach the field in the neighbourhood of this mode would grow in time without bound and would accumulate energy at a constant rate (resonant accumulation of energy). If the system is made dissipative, the growth saturates at values inversely proportional to the damping rate. The energy flux to the plasma remains the same irrespective of the damping rate and one talks about resonance absorption. The wave forms for three different dampings $\delta = 162,54,18$ introduced via[38]

$$\vec{\vec{\epsilon}}^{(0)} \longrightarrow \vec{\vec{\epsilon}}^{(0)} + \begin{pmatrix} i\delta & -\delta & 0 \\ \delta & i\delta & 0 \\ 0 & 0 & 0 \end{pmatrix} \qquad (28)$$

are shown in Fig. 6a. The antenna is situated on the right side which is the high magnetic field side (HFS). The incoming fast wave has roughly the same amplitude in all three cases and the power emitted by the antenna is comparable too.

Fig. 6a can be reinterpreted as a time sequence of wave forms. If, in an undamped system, we would find a wave form like the one in the middle at time t = 1 we should have seen the wave form at the top at t = 1/3 and would expect to find that in the bottom graph at t = 3.

In Fig. 6b we show that the energy is convected away from the resonance by the kinetic wave when the hot plasma model is used. We have achieved the same spatial scales at the resonance as in Fig. 6a by using the unrealistic temperatures 90, 10 and 1.1 eV. The damping of the kinetic wave has been adjusted in such a way as to have the same damping length in all three cases.

Now imagine a time sequence in a hot plasma with 10 eV. At t = 1/3 the wave form would be that of the cold plasma. In the course of time the characteristic length would, however, shrink and approach the wavelength of the kinetic wave and at this moment the resonant structure of the fast wave would start to emit the kinetic wave. This sequence is illustrated in Fig. 6c where the hot plasma model is used and the damping is changed, δ = 162, 54, 18, representing growing time.

Let us now turn to the 2D situations depicted in Figs. 7-9. These figures have been produced using the Lausanne ION-cyclotron code LION[21] which is based either on the cold or on what we call the "warm" plasma model. In the cold plasma model (Fig. 7) dissipation is provided by Eq. (28) whereas in the "warm" plasma model the ion-cyclotron damping is used in addition (Figs. 8 and 9).

In Fig. 7 the same plasma parameters have been used as in Fig. 6, apart from the plasma current which is unimportant in a plane slab ICRF model but very important for a 2D model where it determines the equilibrium and the geometry of the magnetic field. An analytical Solov'ev equilibrium[39] with q(0) = 1 has been used for simplicity. Fig. 7 corresponds to Fig. 6a; the same three dampings have been used and the result can again be interpreted as a time sequence. As in Fig. 6a the antenna excites the fast magnetosonic wave which suffers from singularities. For graphical reasons only the singular regions are shown in Fig. 7. They are situated on certain magnetic surfaces[3] as predicted analytically.[40,41] In the course of time the incoming fast wave excites the geometrically predetermined resonant structure to higher and higher amplitudes whereby the structure's radial half-widths shrink inversely proportional to the time. The poloidal extension of the structure, however, remains constant, its centre being aligned with the ion-ion hybrid resonance condition

$$\frac{\omega^2}{c^2}\,\epsilon_{nn}^{(0)} = k_{\parallel}^2 \qquad (29)$$

as obtained from the geometric optics and indicated by a broken line in Fig. 7. Here and in the following, the index n denotes the direction normal to the magnetic surfaces. Physically, the resonant structure can be understood as poloidally standing, radially singular Alfven or ion-cyclotron waves or eigenmodes. When modelled by hot physics in analogy to Fig. 6c these modes would start to emit kinetic waves when their radial extension starts to be as small as the wavelength of the latter. It is to be expected that the phase velocity of the kinetic wave would be directed radially as sketched in Fig. 7. If the kinetic wave is not absorbed between individual resonant surfaces complicated standing wave patterns of even the kinetic wave could be set up. These patterns should be strongly temperature dependent.

The academically interesting transition from the present 2D picture back to 1D can be made by either diminishing the equilibrium current or by increasing the plasma size.[3] In both cases the number of resonant surfaces increases and the poloidal extensions of the reso-

nant structure become smaller. In both limits one can recover the 1D picture of a resonant structure defined by Eq. (29).

A large plasma like JET, however, can still be dominated by 2D effects.[42,43] In contrast to Ref. 42 here we show results obtained using the "warm" model for a JET plasma (aspect ratio 2.4, $q(0) = 1$, $q(r_p) = 2.2$, elongation 1.68, $B_0 = 3.4$ T, $R_0 = 3$ m, $n_{eo} = 3.2 \cdot 10^{19} cm^{-3}$, $T_i = 6$ keV, $f_0 = 43$ MHz, $n = -15$) containing a mixture of deuterium and hydrogen with $n_H/n_e = 0.3$ if not stated otherwise.

In Fig. 8 is shown the wave form of a fast wave incident from the low-field side (LFS). In the 1D model this wave encounters a cut-off in front of the resonance. In a large plasma like JET the 1D result obviously has significance. One observes a dominant standing wave structure of the fast wave and a very weak excitation (through tunneling) of the resonant structure described above. If the antenna is situated on the HFS, however, the incident fast wave does not set up a standing wave (Fig. 9, left side) on its way inwards but delivers its energy to the standing resonant structure which in this case is the dominant feature of the wave form.

In Fig. 9 we also show how the wave structure changes with decreasing minority density (from left to right, $n_H/n_{eo} = 0.3$, 0.1, 0.03). At the lowest concentration the ion-cyclotron damping is active even at the ion-ion hybrid resonance and the geometric features due to the cold plasma are completely wiped out. It is only in this limit that one could expect a ray-tracing code[2] to produce reliable results. All the other cases in Figs. 8 and 9 cannot be treated by ray-tracing because it cannot handle standing waves.

6. CONCLUSION

It has been shown that the linear theory of electromagnetic wave propagation in a hot plasma is not completely developed yet. We have, however, found a satisfactorily working version which can be applied

to the whole low frequency range without ad hoc approximations. We have found reasonable definitions for the energy flux and the local absorption. In particular, we have shown that we are able to include transit time magnetic pumping even in cylindrical geometry. In view of the results which are to be expected from the 2D kinetic ICRF codes we have tried to predict some of the main features of mode conversion in two dimensions.

ACKNOWLEDGEMENT

We thank F. Skiff, E. Tennfors and M. Brambilla for discussions. This investigation was partly supported by the Swiss National Science Foundation.

REFERENCES

1 T. Hellsten and K. Appert, Proc. 13th Europ. Conf. on Contr. Fusion and Plasma Heating, Schliersee, Europhys. Conf. Abstr., Vol. 10C, part II, p. 129.

2 M. Brambilla, Computer Phys. Rep. 4 (1986) 71.

3 K. Appert et al., Plasma Phys. and Contr. Fusion 28 (1986) 133.

4 T. Martin and J. Vaclavik, "Dielectric tensor operator of a nonuniformly magnetized inhomogeneous plasma", Lausanne report, LRP 259/85, Helv. Phys. Acta 60 (1987) 471.

5 A. Hasegawa and L. Chen, Phys. Rev. Lett. 35 (1975) 370.

6 D.L. Grekov, K.N. Stepanov and J.A. Tataronis, Sov. J. Plasma Phys. 7 (1981) 411.

7 T.H. Stix, Proc. 2nd Joint Grenoble-Varenna Int. Symp., Heating in Toroidal Plasmas, Como 1980; CEC Brussels 1981, Vol. II, p. 631.

8 D.W. Ross, G.L. Chen and S.M. Mahajan, Phys. Fluids 25 (1982) 652.

9 K. Itoh and S.-I. Itoh, Plasma Phys. 25 (1983) 1037.

10 I.J. Donnelly, B.E. Clancy and N.F. Cramer, J. Plasma Phys. 35 (1986) 75.

11 T.H. Stix and D.G. Swanson. In M.N. Rosenbluth and R.Z. Sagdeev (Ed.), Handbook of Plasma Physics, Vol. 2. North-Holland Publishing Company, Amsterdam, Ch. 2.4.

12 D.L. Grekov et al., Proc. 2nd Grenoble-Varenna Int. Symp., Heating in Toroidal Plasmas, Como 1980; CEC Brussels 1981, Vol. I, p. 519.

[13] A.M. Messiaen et al., Nucl. Fusion 15 (1975) 75.

[14] P.L. Colestock and R. Kashuba, Nucl. Fusion 23 (1983) 763.

[15] S.C. Chiu and T.K. Mau, Nucl. Fusion 23 (1983) 1613.

[16] A. Fukuyama et al., Nucl. Fusion 23 (1983) 1005.

[17] B.D. McVey, R.S. Sund and J.E. Scharer, Phys. Rev. Letters 55 (1985) 507.

[18] J. Vaclavik and K. Appert, Plasma Phys. and Contr. Fusion 29 (1987) 257.

[19] G. Strang and G.J. Fix, "An analysis of the finite element method", Prentice-Hall, Englewood Cliffs, 1973.

[20] K. Appert, T. Hellsten, J. Vaclavik and L. Villard, Comput. Phys. Commun. 40, (1986) 73.

[21] L. Villard, K. Appert, R. Gruber and J. Vaclavik, Comput. Phys. Reports 4, (1986) 95.

[22] T.H. Stix, "The theory of plasma waves", McGraw-Hill, New York, 1962.

[23] K. Appert, S. Succi, J. Vaclavik and L. Villard, "Finite elements applied to plasma waves", Lausanne report, LRP 304/86, accepted for publication by Comput. Phys. Reports.

[24] V.D. Shafranov, in Reviews of Plasma Physics, edited by M.A. Leontovich, Consultants Bureau, New York, 1967, Vol. 3.

[25] K. Appert and J. Vaclavik, Plasma Physics 25, (1983) 551.

[26] K. Appert, J. Vaclavik and L. Villard, Lecture Notes, "An introduction to the theory of Alfvén Wave Heating", Lausanne report LRP 238/84, 1984.

[27] O.S. Burdo et al., Sov. J. Plasma Phys. 9, (1983) 403.

[28] I.J. Donnelly, B.E. Clancy and M.H. Brennan, Proc. 13th Europ. Conf. on Contr. Fusion and Plasma Heating, Schliersee, Europhys. Conf. Abstr., Vol. 10C, part I, p. 431.

[29] G.A. Collins et al., Phys. Fluids 29, (1986) 2260 and references cited therein.

[30] J.B. Lister, paper invited to this Conference.

[31] K. Appert, J. Vaclavik and L. Villard, Phys. Fluids 27, (1984) 432.

[32] K. Appert and J. Vaclavik, "Energy transfer from standing waves to gyrating particles", LRP 310/86; paper contributed to this Conference.

[33] A. de Chambrier et al., Proc. 3rd Joint Varenna-Grenoble Int. Symp., Heating in Toroidal Plasmas, Grenoble 1982; CEC Brussels, 1982, Vol. I, p. 161.

[34] A. de Chambrier et al., Phys. Letters 92A, (1982) 279.

[35] S. Puri, Proc. 2nd Joint Grenoble-Varenna Int. Symp. Como 1980; CEC Brussels, 1981, Vol. II, p. 671.

[36] K. Appert et al., Phys. Rev. Letters 54, (1985) 1671.

[37] L.A. Artsimowitsch und R.S. Sagdejew, "Plasmaphysik für Physiker", Teubner, Stuttgart, 1983; from Russian "Fizika plasmy dlia fizikov", Atomizdat, Moskva, 1979.

[38] O. Sauter et al., "Numerical modelling of the ion-ion hybrid resonance", Lausanne report, LRP 316/87, 1987, note submitted to Comput. Phys. Commun.

[39] L.S. Solov'ev, Sov. Phys.-JETP 26, (1968) 400.

[40] T. Hellsten and E. Tennfors, Physica Scripta 30, (1984) 341.

[41] E. Tennfors, Plasma Phys. Contr. Fusion 28, (1986) 1483.

[42] L. Villard et al., "Global waves in the ICRF in JET plasmas", LRP 310/86, paper contributed to this Conference.

[43] O. Sauter et al., "HFS and LFS scenarii for ICRF heating in JET", LRP 310/86, paper contributed to this Conference.

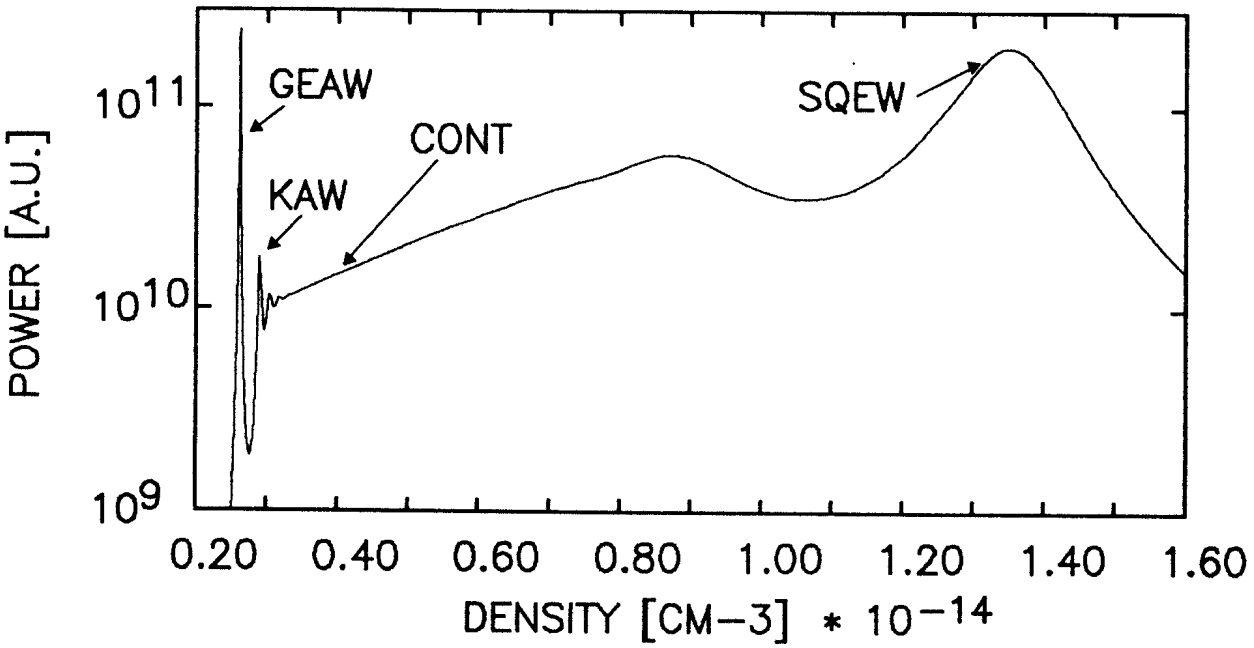

Fig. 1: Power versus central electron density for TCA with m = -1 and n = -2.

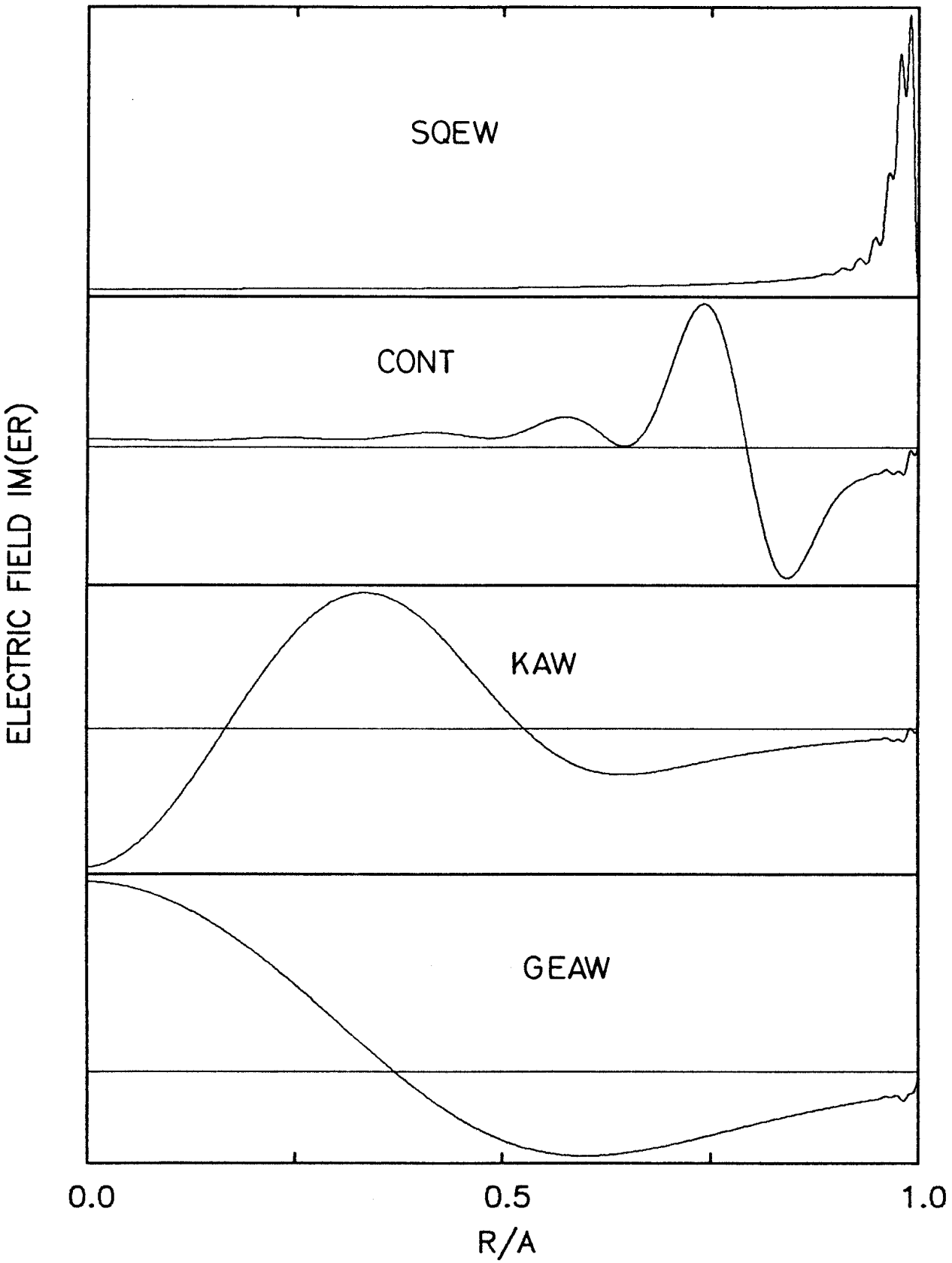

Fig. 2: Typical wave forms in different regimes defined in Fig. 1. Shown are the imaginary parts of the radial component of the wave electric field versus radius.

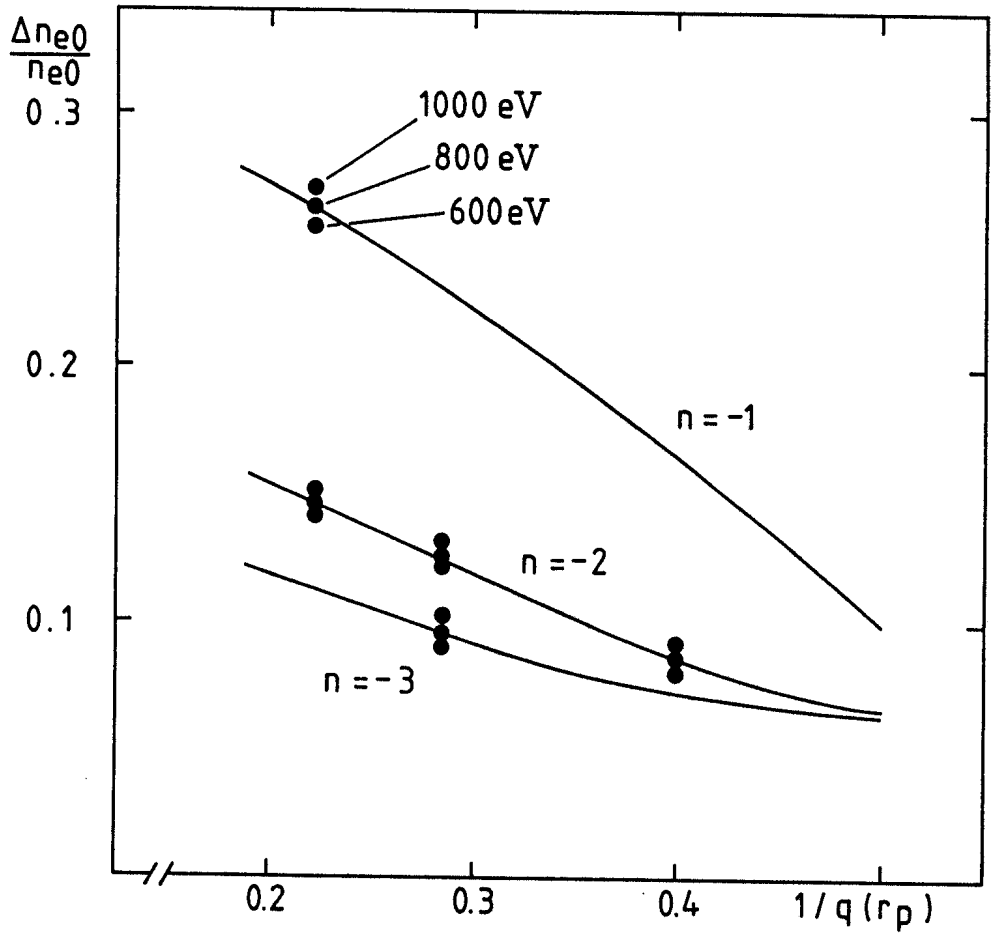

Fig. 3: Relative distance between the GEAW and the KAW versus the plasma current for 3 different toroidal wave numbers and 3 different temperatures, the solid lines corresponding to 800 eV.

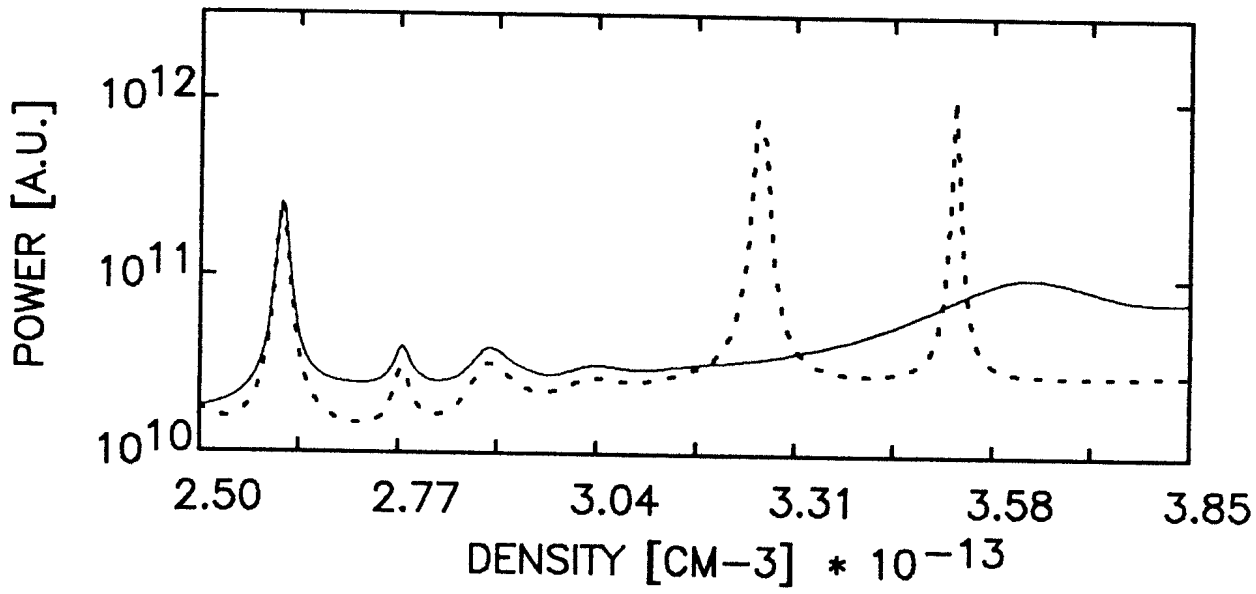

Fig. 4: Total power due to the 4 modes with $|m| = 1$ and $|n| = 2$ versus central electron density for TCA. Two different temperatures at the plasma boundary are used: $T_{eo} = 2$ eV, broken line, $T_{eo} = 20$ eV, solid line.

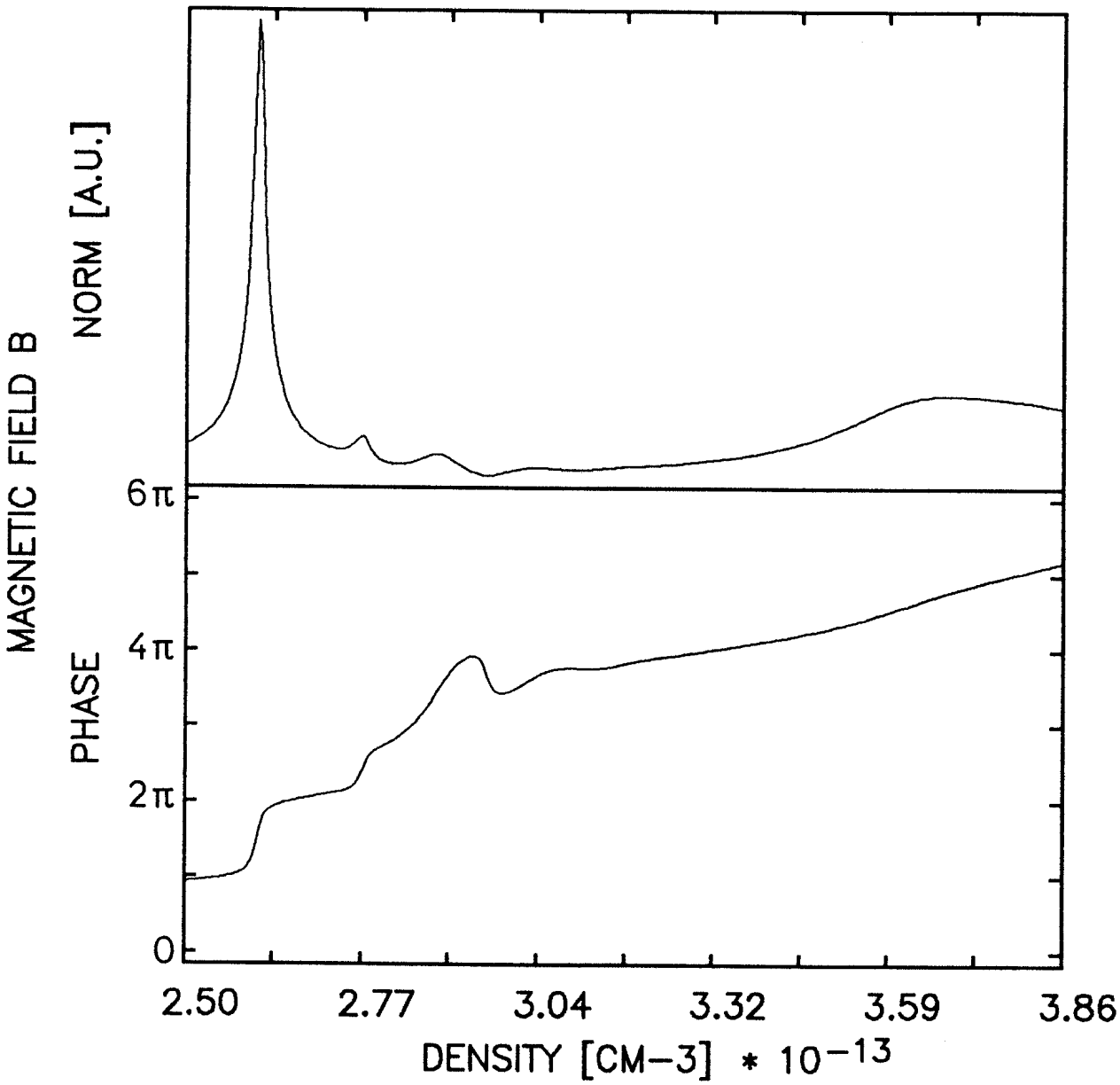

Fig. 5: Absolute value and phase of vacuum wave magnetic field $B_{\parallel}$ versus density. Parameters are the same as in Fig. 4.

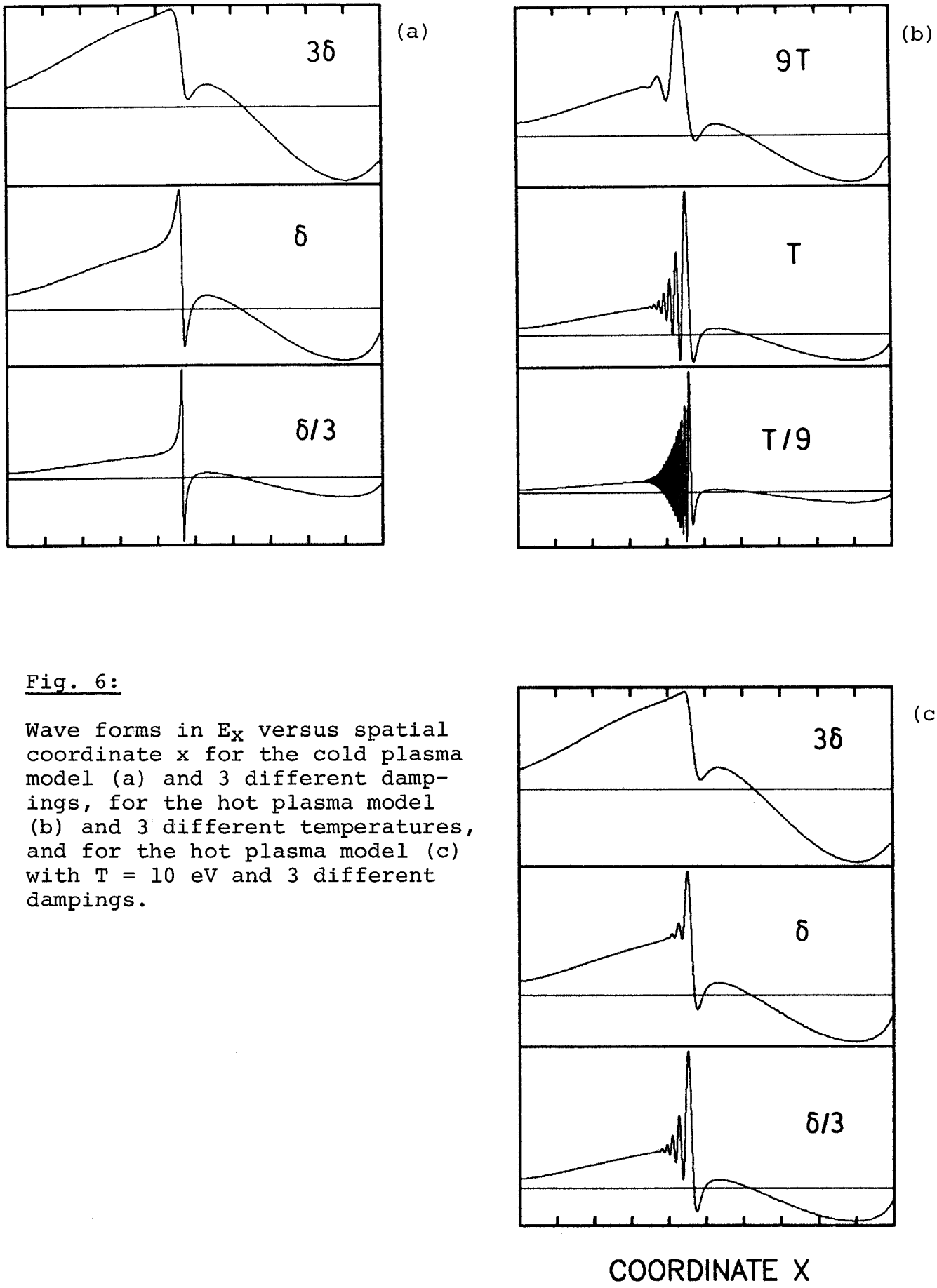

Fig. 6:

Wave forms in E_x versus spatial coordinate x for the cold plasma model (a) and 3 different dampings, for the hot plasma model (b) and 3 different temperatures, and for the hot plasma model (c) with T = 10 eV and 3 different dampings.

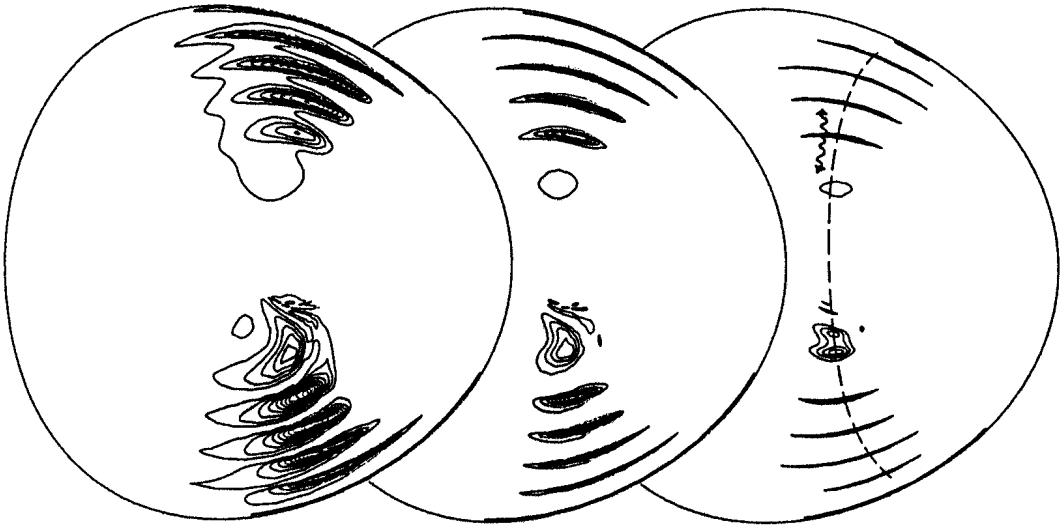

damping :	3	1	1/3
or			
"time" :	1/3	1	3

Fig. 7: Equilines of the power absorption density in a TCA plasma for 3 different dampings corresponding to those used in Fig. 6.

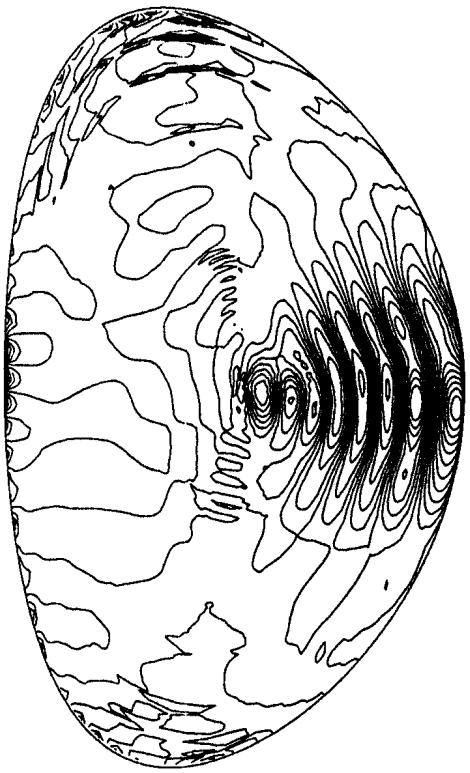

Fig. 8:

Equilines of $Re(E_n)$ in a "warm" D/H JET plasma with LFS excitation.

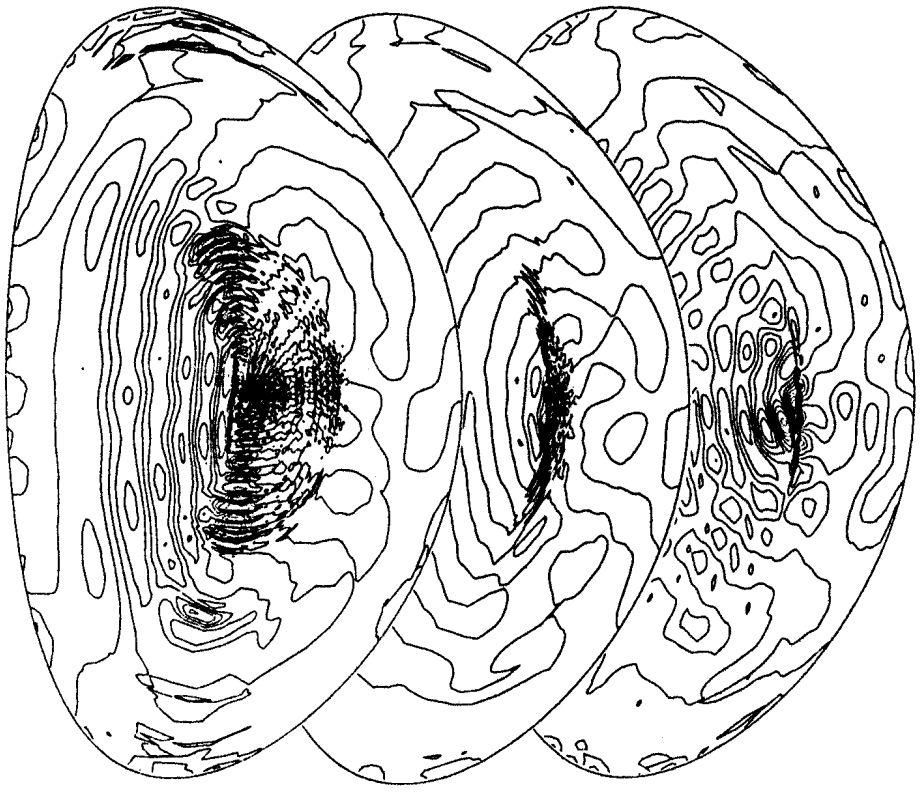

Fig. 9: Equilines of $Re(E_n)$ in a "warm" JET plasma with HFS excitation and varying H minority concentration (from the left to the right, n_H/n_{eo} = 0.3, 0.1, 0.03).